Journal of Macromolecular Science, Part A
Publication details, including instructions for authors and subscription information:
http://www.informaworld.com/smpp/title~content=t713597274

Characterization of Naturally Weathered Polypropylene Plates

R. Gallo[a]; L. Brambilla[b]; Chiara Castiglioni[b]; F. Severini[b]
[a] Dipartimento di Chimica Industriale e Ingegneria dei Materiali, Università di Messina, Salita Sperone, Sant'Agata di Messina, Italy [b] Dipartimento di Chimica, Materiali e Ingegneria Chimica "G. Natta", Politecnico di Milano, Piazza Leonardo da Vinci, Milano, Italy

To cite this Article Gallo, R. , Brambilla, L. , Castiglioni, Chiara and Severini, F.(2006) 'Characterization of Naturally Weathered Polypropylene Plates', Journal of Macromolecular Science, Part A, 43: 3, 535 — 554
To link to this Article: DOI: 10.1080/10601320600575280
URL: http://dx.doi.org/10.1080/10601320600575280

Journal of Macromolecular Science®, Part A: Pure and Applied Chemistry, 43:535–554, 2006

ISSN 1060-1325 print/1520-5738 online
DOI: 10.1080/10601320600575280

Characterization of Naturally Weathered Polypropylene Plates

R. GALLO,[1] L. BRAMBILLA,[2] C. CASTIGLIONI,[2]
AND F. SEVERINI[2]

[1]Dipartimento di Chimica Industriale e Ingegneria dei Materiali,
Università di Messina, Salita Sperone, Sant'Agata di Messina, Italy
[2]Dipartimento di Chimica, Materiali e Ingegneria Chimica "G. Natta",
Politecnico di Milano, Piazza Leonardo da Vinci, Milano, Italy

The natural outdoor ageing of thick plates of isotactic polypropylene is investigated. Different techniques (infrared spectroscopy, thermal analysis, scanning electron microscopy, and mechanical tests) are used in order to obtain a comprehensive view of the modifications occurring during the environmental ageing. The degradation of the material is ascribed to a morphology variation, with relevant changes in the crystallinity percentage. At any exposure time, the degree of oxidation shows a marked decrease while passing from the material near to the surfaces to the material of the inner regions. This suggests that other chemical reactions different from oxidation are responsible for the polymer degradation in the inner region of the plates.

Keywords infrared spectroscopy, thermal analysis, isotactic polypropylene, natural degradation

Introduction

Studies on isotactic polypropylene (iPP) degradation in natural environment are relatively few with respect to laboratory experiments carried out by irradiation of iPP samples with ultra-violet light of constant intensity in a controlled atmosphere. The results obtained with outdoor natural exposure are different while varying the place of exposure, but are very important in order to define the average lifetime of the polymer in a given natural environment and to establish the more suitable stabilizers (1, 2). The environmental weathering is the result of combined chemical and physical reactions, for instance, photochemical reactions associated to photons of different energies; mechanical actions of wind, rain and powders; thermal cycles associated to day and night alternation. These last effects can induce non-negligible changes in the polymer at the morphological level.

Not all effects of the natural weathering are predictable. For instance, Tidjani (3) found that low crystallinity iPP keeps its mechanical characteristics for a longer time with respect to materials obtained from a highly crystalline polymer. Most of the works

Received May 2005; Accepted July 2005.

Address correspondence to Chiara Castiglioni, Dipartimento di Chimica, Materiali e Ingegneria Chimica "G. Natta", Politecnico di Milano, Piazza Leonardo da Vinci, 32, 20133; Milano, Italy. Tel.: ++39 02 23993230; Fax: ++39 02 23993231; E-mail: chiara.castiglioni@polimi.it

on the iPP degradation (both in a natural environment and in the laboratory) are based on experiments on films of thickness between 25 and 500 μm (4–7), while the natural degradation process of plates (thickness larger than 1 mm) is rarely investigated. On the other hand, these kinds of studies are welcome, due to the fact that the behavior of thick samples would better reproduce what happens in practical applications products (2, 8). Bedia et al. studied the weathering of 2 mm thick iPP samples in a tropical zone. They found that the degradation processes accompanied by a lowering of the molecular weight involve all the polymer mass, already at very short exposure times. However, the material in the proximity of the surface directly exposed to the sunlight is more affected by degradation. Castejon et al. (4, 5) studied the thermal and photochemical degradation of iPP sheets with a thickness of 0.5 mm with laboratory experiments. In this work, Differential Scanning Calorimetry has been widely used in order to follow the polymer changes while increasing the weathering process. In the first 100 h, the authors observe a marked decrease of the molecular weight, followed by a very smooth decrease in the subsequent 2000 h of weathering. It has been observed that the degree of crystallinity systematically decreases with the exposure time. This result is in agreement with the behavior observed for a thin iPP film photo-degraded by exposure in a natural environment (7), but differs from what is found in the case of the natural weathering of thick (2 mm thickness) iPP plates (2). In this last case, a non-monotonic variation of the crystallinity percentage has been observed, consisting of a first increase, followed by a plateau and then by a decrease at a higher length of (10 months) exposure.

Several investigations (9, 10) (mainly carried out with laboratory experiments) stress the importance of the sample thickness in determining the course and the characteristic of the photo-oxidation of iPP. It is interesting to notice that similar changes in the polymer molecular weight are obtained after similar exposure times (2.5 months) both for a thin film (26 μm) (6) and for a thick sheet (2 mm) (2).

In our previous works (6, 7), we reported the results obtained by studies on iPP degradation in a natural environment, as derived by experiments on thin samples (26 and 50 μm thick).

In this work, we present a study of the natural weathering of iPP samples 2 mm thick, exposed outdoors in the same place. These samples have been obtained by compression molding of polymer granules without a light stabilizer. The polymer used contains a very low amount soluble in heptane and a crystallinity percentage of 41%, measured by thermal analysis on the starting material (plate) on the basis of the melting enthalpy, by comparison with the ideal value for a 100% crystalline iPP ($\Delta H = 209\,J\,g^{-1}$) (11).

This work is intended to clarify some of the problems not yet solved which are related to the thermal and photochemical processes and to the consequent morphology changes, which take place during the natural weathering of iPP.

Experimental

Experiments were carried out on 2 mm plates of isotactic polypropylene prepared by compression molding at 190°C for two minutes with a 20 bar pressure. The polypropylene used is a commercial material (Moplen T 30 S supplied by Monteshell s. p. a.) containing a very low quantity of process stabilizer and not stabilized to light. The polymer melt index was 3.3 g/10 min (ISO 1133) and average molecular weight $M_w = 441000$ dalton. The melting and crystallization enthalpy determined by DSC analysis were $85.6\,J\,g^{-1}$ and $97.7\,J\,g^{-1}$, respectively. The exposure tests started in January 2000 at Messina (Italy) (38° 11′ 20″ north, 15° 33′ 30″ east; 59 m from sea level). In this place, the number of rainy days was 150 for a year with 762 mm of annual rainfall and the windy days were about 75%, with winds mainly from S and SW (12). The plates were mounted on wooden frames inclined at 45° with respect to the horizon and were exposed facing southwest on a terrace at about 20 m above the ground. Several techniques were used in order to follow the degradation process with ageing time: differential scanning calorimetry (DSC), thermo-gravimetric analysis (TGA), scanning electron microscopy (SEM), Fourier transform infrared spectroscopy (FT-IR) and mechanical tests.

DSC curves were obtained on a DSC-2 Perkin-Elmer instrument using aluminium pans under nitrogen. Indium was used as the standard for calibrating the temperature axis and the enthalpy output. The weight loss of the pristine plate and of the aged samples was obtained by dynamical thermogravimetric analysis (TGA) with a TGS-2 Perkin-Elmer thermo-balance in air with a heating rate of 20 deg $\min^{-1}$ in the range 323–1223 K.

Scanning electron microscopy experiments have been carried out with a Zeiss DSM 490 instrument. Attenuate total reflection (ATR) infrared spectra have been recorded with a Nicolet Magna 560 interferometer, using a 45° shaped KRS5 ATR crystal, with the exception of the case of the sample withdrawn after 816 h of exposure where a 45° shaped Germanium crystal has been used; the angle of incidence of the IR beam on the sample was 45° in all the ATR experiments. Absorption infrared experiments have been carried out on powders scratched from samples exposed for 4896 h, 6624 h, and 11640 h respectively and dispersed in KBr pellets.

Mechanical tests of a few samples have been performed on an Instrom tensile testing machine 1115 at a traction rate of 500 mm/min, at 25°C and 50% humidity.

Results and Discussion

Mechanical Tests

After 4000 h exposure time, the plate was characterized by a yield strength very close to that of the non-exposed sample (0 h), but the elongation at rupture dramatically decreases. Samples exposed for 6024 h could be broken by finger deformation even if it showed a good surface. After 11640 h of exposure, the plate was very brittle and strongly chalked. In Table 1, the data relative to the mechanical tests are reported. These data can be compared with those obtained by artificial degradation of thick polypropylene samples reported in literature (13, 14).

Microscopy Analysis

The surface and section morphology of polypropylene plates exposed for different times were observed by means of Scanning Electron Microscopy.

Table 1

Data obtained by mechanical tests on exposed and unexposed iPP samples

Sample	Yield strength (Mpa)	% Elongation at breaking
Not exposed	36	528
After 4000 h. exp. time	36	17

SEM images at low magnification (×200) of the surfaces (Figure 1) after 3648 h of exposure shows a dense net of micro-fractures on a flat surface. At higher times of exposure, when the ageing starts to also involve the inner material, the surface morphology appears heavily affected (Figure 2).

In order to have a qualitative evaluation of the penetration of the degradation process, sections of the specimens were observed by SEM microscopy. The sections of the pristine plate and of the aged samples were made by breaking after cooling in liquid nitrogen. In Figure 3 we can see a section (magnification ×50) of the unexposed sample. The image looks homogenous along the entire section, showing an almost uniform grey color.

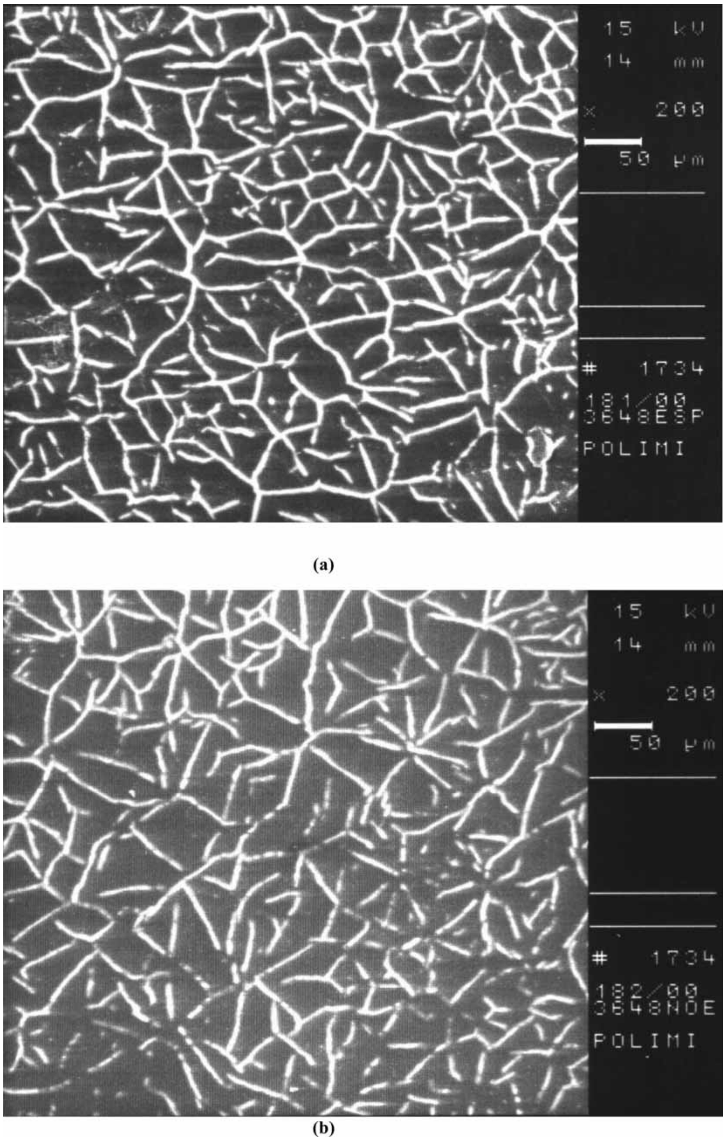

Figure 1. SEM image (200 X magnification) of the upper (a) and of the lower (b) surface of a plate of iPP after 3648 h of exposure.

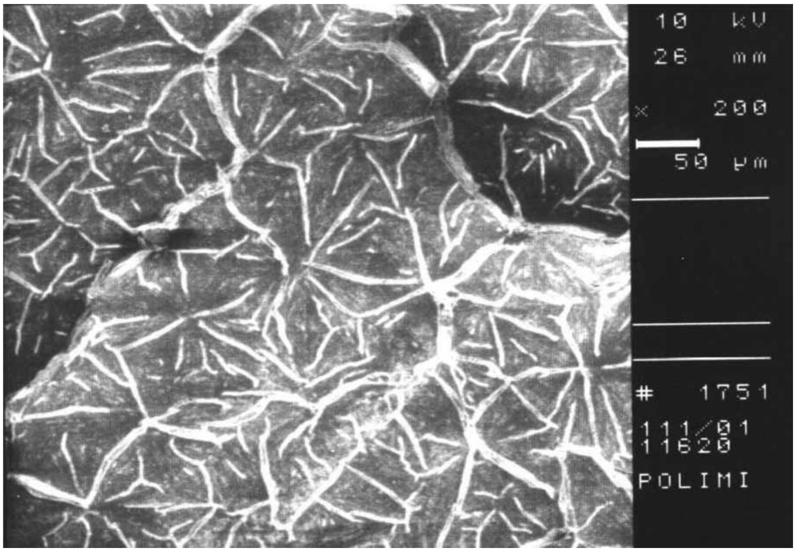

Figure 2. SEM image (200 X magnification) of the upper surface of a plate of iPP after 11620 h. of exposure.

The section after 2520 h (Figure 4) shows differences in the regions close to the two surfaces of the plate. The material close to the surface directly exposed to the sunlight (upper surface in the picture) shows white regions and some indication of erosion, while near the lower surface, it shows a more homogeneous color with several micro-fractures, but to a lesser extent.

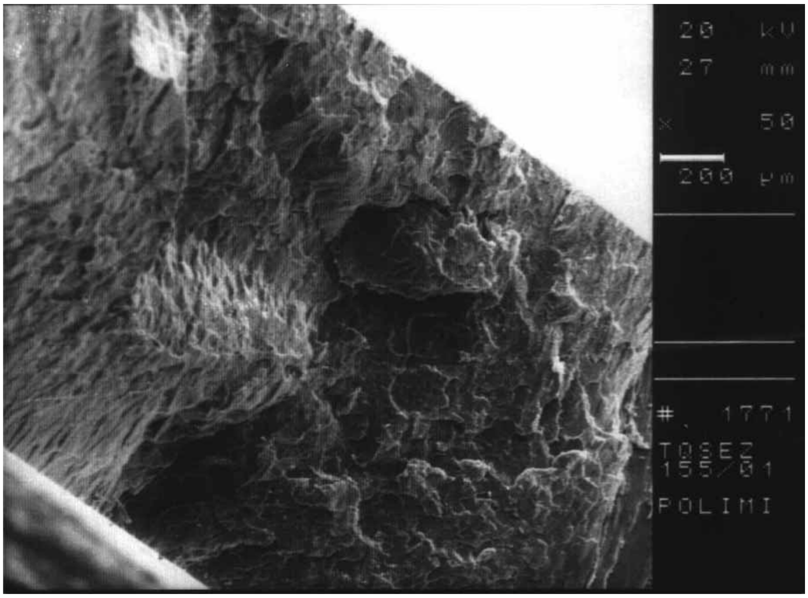

Figure 3. SEM image (50 X magnification) of a section of a pristine (0 h. exposure time) plate of iPP.

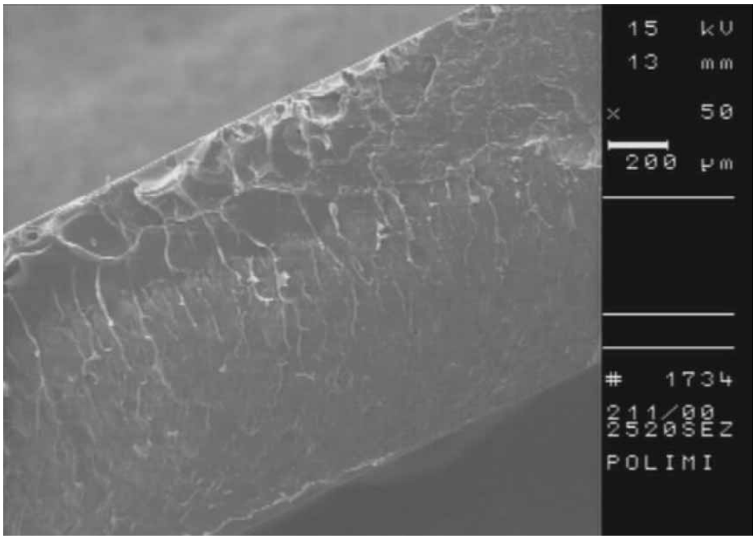

Figure 4. SEM image of a section of a plate of iPP after 2520 h. of exposure. a: 50 X magnification.

The section of the sample withdrawn after 3648 h (Figure 5), shows a deeper penetration of the white structures under the exposed surface; also in this case, the lower surface appears to be more homogenous. Differences between the two regions (near the upper and near the lower surface of the plate) become less pronounced in the sample withdrawn after 4896 h (Figure 6), where white structures appear on both sides. The highly degraded sample of Figure 7 (11620 h) shows fractures to a large extent; regions near the two opposite surfaces are no longer distinguishable.

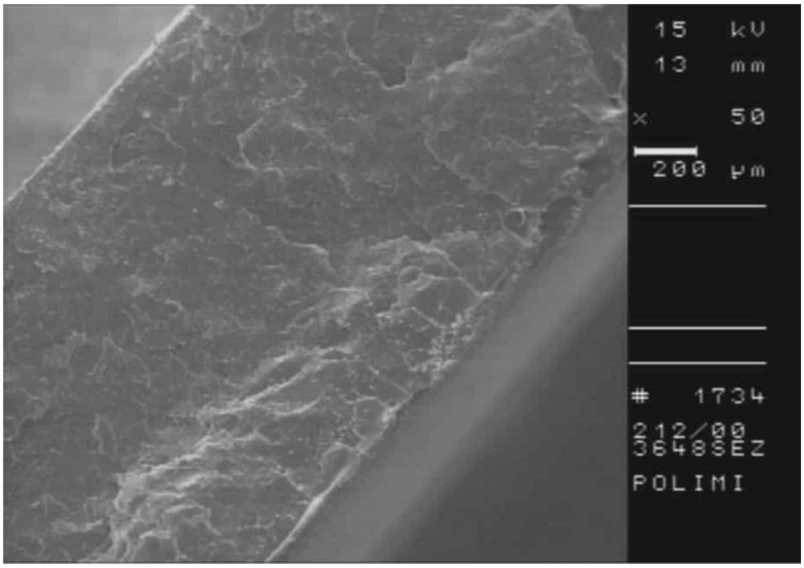

Figure 5. SEM image (50 X magnification) of a section of a plate of iPP after 3648 h. of exposure.

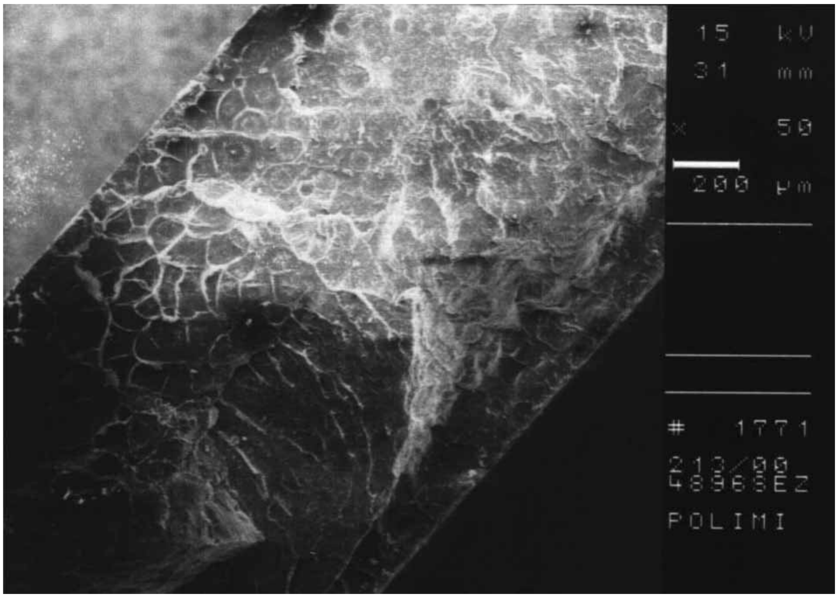

Figure 6. SEM image (50 X magnification) of a section of a plate of iPP after 4896 h. of exposure.

Infrared Experiments

In order to study the chemical and morphological modifications induced during the outdoor exposure on the iPP plates, ATR and absorption infrared analysis on samples exposed for 0, 816, 2520, 4696, 4896, 6624, and 11640 h have been carried out.

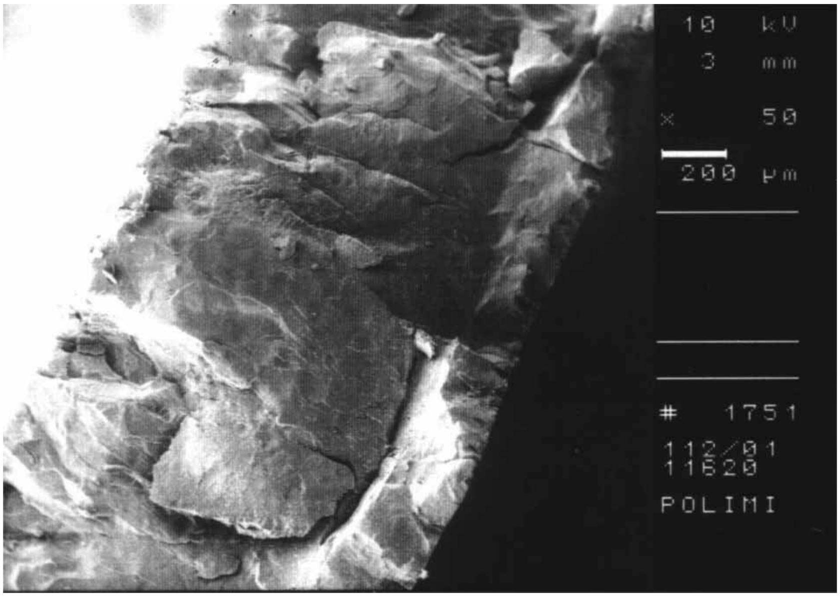

Figure 7. SEM image (50 X magnification) of a section of a plate of iPP after 11620 h. of exposure.

ATR Experiments

In Figure 8, we report two different ATR spectra of the same unexposed sample before (spectrum a) and after (spectrum b) cleaning of the surface with acetone: in Figure 8, the difference spectrum is also reported (c). In the spectrum (a) we observe, together with bands characteristic of the crystalline isotactic polypropylene (15–17), some new bands highlighted in the difference spectrum (c): these bands must be inevitably attributed to chemical species different from iPP, namely silicon oils used as a detaching agent in the molding process. All these extra bands virtually disappear in the spectrum of cleaned sample (see spectrum b), thus indicating that the unknown chemical substances are deposited on the surface.

In the spectra of the exposed samples, extra peaks at 1650, 1018, 797 and 461 cm^{-1} are clearly observed: these bands indicate the presence of silica and calcium carbonate on the surfaces of the plates (probably micro particles of the Saharan sand carried by winds) and disappear after cleaning the surfaces. The surfaces of the exposed samples have been gently cleaned with a cotton wool soaked with acetone, in order to remove both the silicon oils and the dust deposited on the surfaces: this procedure enables us to achieve a good samples contact with the ATR crystal.

In the work of Carlsson et al. (18), the degree of photo-oxidation of thin iPP films has been investigated by ATR experiments at various controlled penetration depth. The same technique has been used in this work in order to detect signals from oxidation at the beginning of the exposure.

Indeed, to investigate a region of the sample very close to the surface, ATR spectra of the plate which was withdrawn after 816 h have been recorded using a Germanium ATR crystal, which ensures a very low depth of analysis (18). This is especially valuable for samples, which have been exposed for short times, since we expect that the degradation, at least in its first stage, mainly involves the sample surfaces. The recorded spectra do not

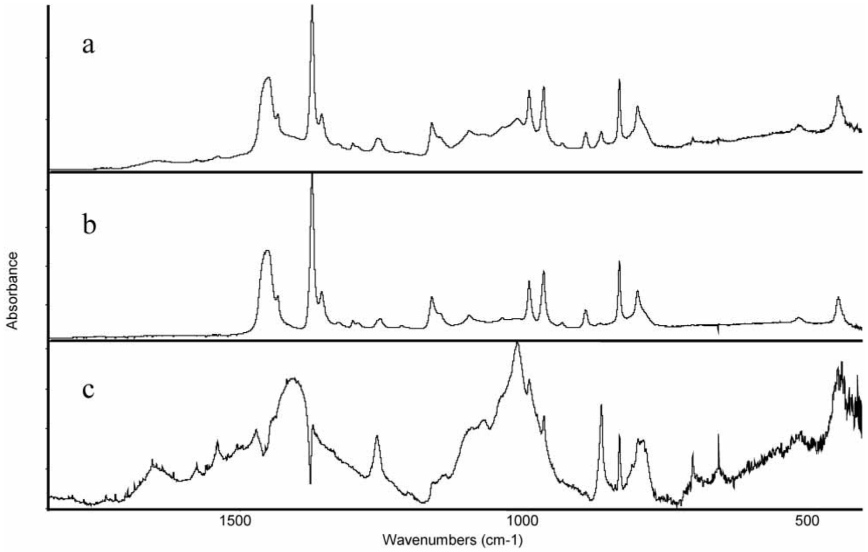

Figure 8. Infrared ATR spectra of a sample (iPP plate) at 0 hours of exposure, before (a) and after (b) cleaning the surface with acetone; (c) spectrum difference.

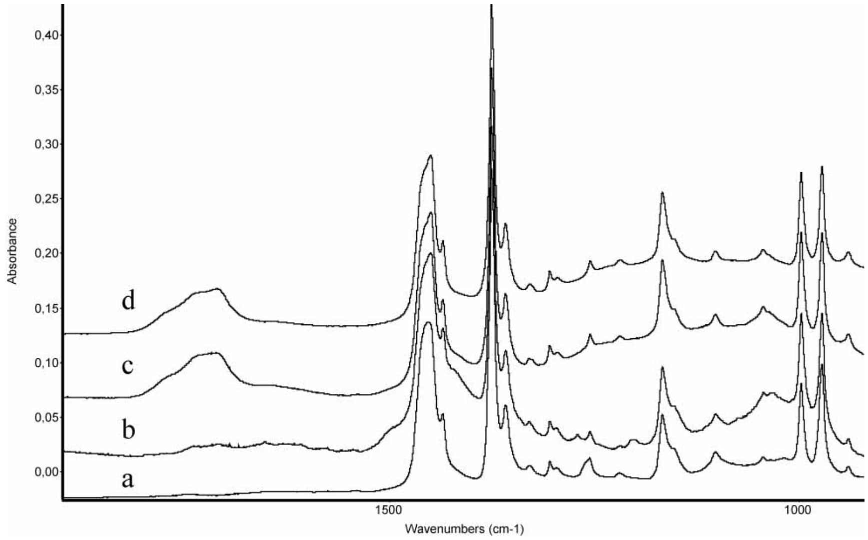

Figure 9. Infrared ATR spectra of the directly exposed surfaces of iPP samples after 0 (a), 2520 (b), 4696 (c) and 6624 h (d) of exposure.

show any feature attributable to degradation processes (e.g., oxidation bands) involving the polymer: only at a higher time, the oxidation processes start showing the presence of new bands near 1700 cm^{-1}.

Figure 9 reports the spectra of the directly exposed surfaces of samples withdrawn after 0, 2520, 4696, and 6624 h. In the spectrum (9b) of the 2520 h sample, a new broad band assigned to C=O stretching vibrations arises at about 1700 cm^{-1}. The spectrum of the opposite surface shows the same C=O band, but with a lower intensity: this indicates that, at this stage of ageing, the oxidation is more effective on the surface directly exposed to the sunlight. In spectra (9c) and (9d), the C=O stretching absorption bands are clearly detectable; also in these cases, the rear surfaces shows a C=O bands with a lower intensity.

A direct comparison between the spectra recorded at 4696 and 6624 h do not show differences in the intensity of the C=O stretching bands, thus indicating that at this time the oxidation processes on the surfaces have reached a plateau.

In order to follow the evolution of the oxidation process in a more quantitative way, we have evaluated the ratios between the intensity of the C=O stretching bands and that of the methyl symmetric bending bands at 1375 cm^{-1} for the two surfaces (Figure 10: set a and b). These data show that the oxidation process on the surfaces starts after an initial induction time (about 1000 h) and rapidly proceeds reaching a plateau after about 4696 h. As already noticed, the rear surface shows a slightly lower content of C=O groups with respect to that directly exposed. At exposure times higher than 6624 h, ATR analysis becomes unfeasible due to the poor contact between the heavily degraded surfaces and ATR crystal.

Information on the variation of the crystallinity percentage induced by the outdoor exposure can be obtained by analyzing the bands at 997 and 972 cm^{-1}: the first band is a regularity band (16) characteristic of the crystalline iPP, whereas the second one is due both from crystalline and amorphous iPP phases (16, 17). This happens because the

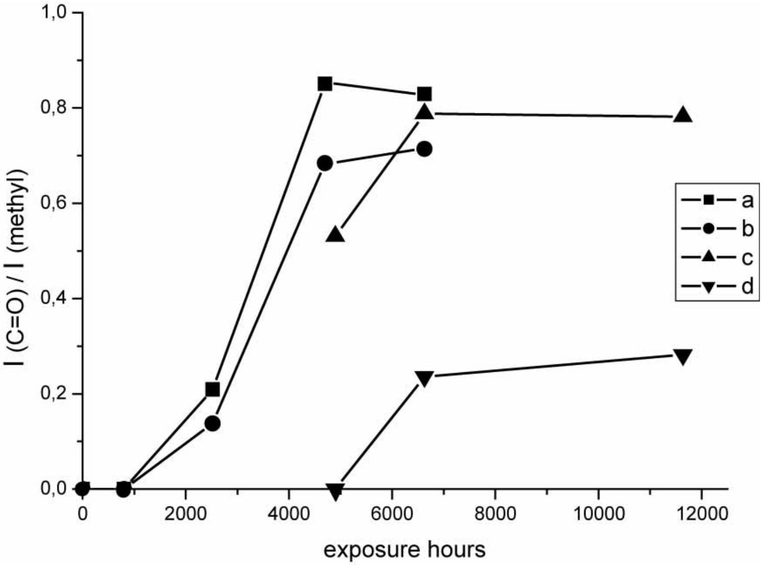

Figure 10. (a) Plot of the ATR infrared intensity ratios between C=O stretching and methyl symmetric bending bands for the two surfaces, (a) and (b), of samples at different ageing times; plot of the same ratios from absorption experiment on (c) surfaces and (d) inner regions.

vibration, which corresponds to the band at 972 cm^{-1} is largely localized on the methyl group and is not influenced by the chain conformation (16). In Figure 11, the evolution of these features with the exposure time is shown by direct comparison of the spectra of iPP samples exposed for 0 and 6624 h, respectively. In the spectrum at 6624 h, the 997 cm^{-1} band is stronger than the corresponding band of the unexposed sample, thus

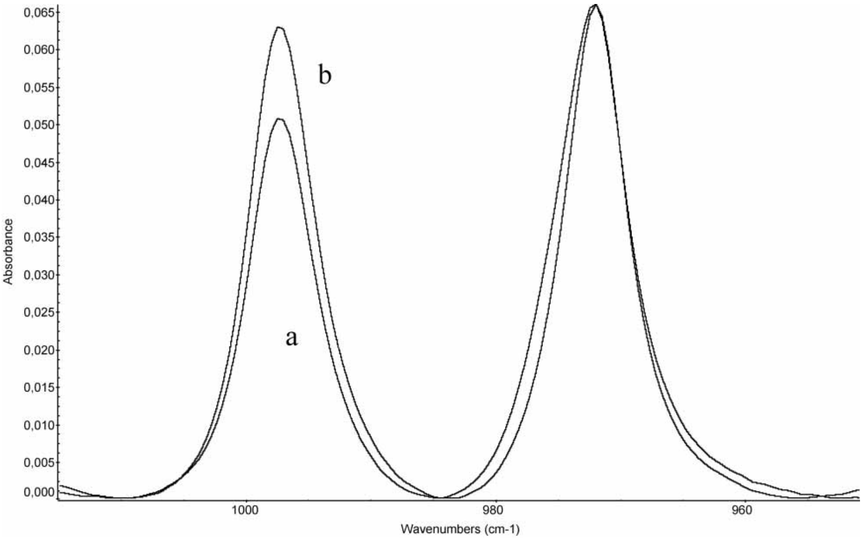

Figure 11. ATR spectra of (a) unexposed and (b) 6624 h exposed iPP in the region of regularity bands.

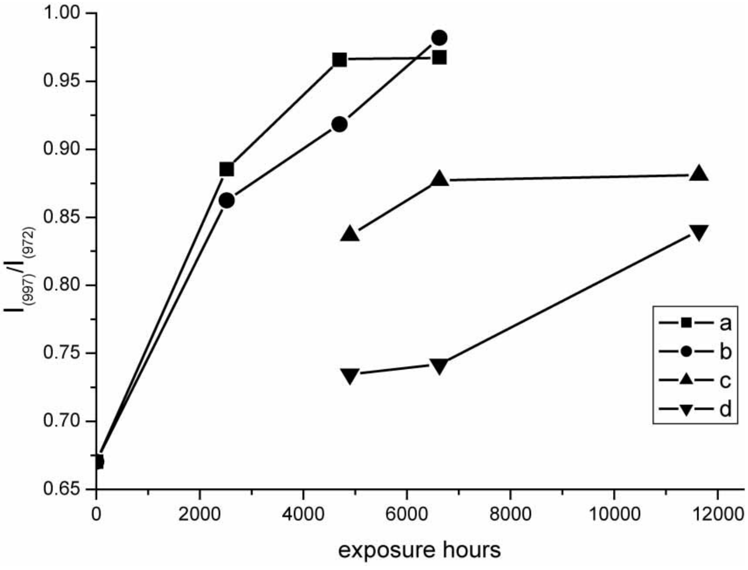

Figure 12. Plot of the ATR infrared intensity ratios between 997 cm^{-1} and 972 cm^{-1} bands for the two surfaces (a: top surface) and (b: bottom surface) of samples at different ageing times; plot of the same ratios from absorption experiment on (c) surfaces and (d) inner regions.

indicating an increase of the relative amount of the crystalline phase. The values of the intensity ratios of these two bands are reported in Figure 12 (sets a and b) for the series of samples examined: the trend obtained indicates that the crystallinity percentage systematically increases on both the surfaces while increasing the exposure time: in the case of exposed surfaces, a plateau is reached after 4696 h.

Absorption Experiments

In order to qualitatively evaluate the penetration of the oxidation processes through the thickness of the plates, the absorption spectra on powders scratched from the exposed surfaces and from the inner regions of samples withdrawn after 4896, 6624, and 11640 h have been recorded.

In the spectra of the surface powders, it can be seen that the C=O stretching region, after an initial rise in absorption intensity, remains practically constant between 6624 h and 11640 h. This suggests that the oxidation processes reach a plateau after about 6600 h.

The spectra obtained from the powders scratched from the inner regions of the samples clearly show that, until 4896 h of exposure, no oxidations signals can be detected. At a higher time the absorption at 1700 cm^{-1} increases with increasing the time of exposure. The intensity ratios between C=O stretching and methyl symmetric bending absorption bands are reported in Figure 10, (sets c and d).

In Figure 12 (sets c and d) the intensity ratios between 997 cm^{-1} and 972 cm^{-1} bands, obtained from absorption experiments are reported. The material near the surfaces shows a plateau in the crystallinity percentage at about 6600 h. On the contrary, an increasing trend is found for the materials taken from the inner regions of the plates.

Some interesting observations can be made considering band shapes in the different spectra: the material near the exposed surface has bands sharper and more symmetric

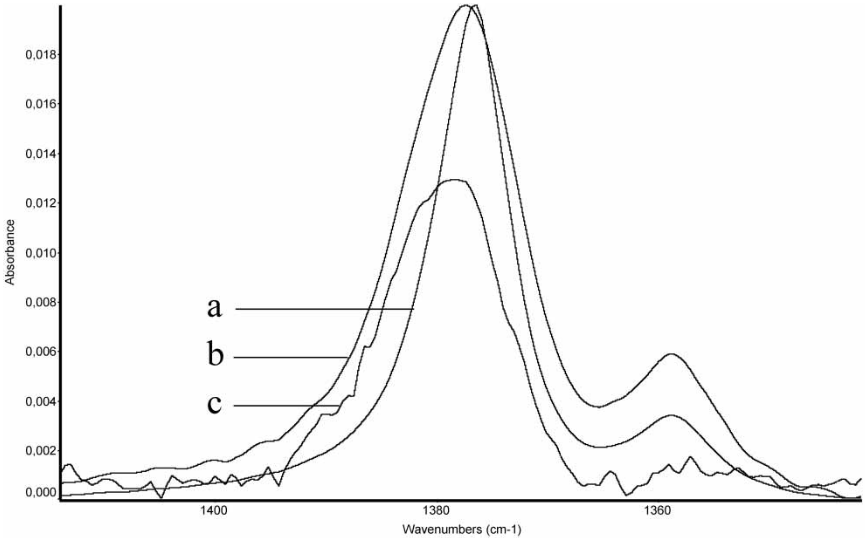

Figure 13. Infrared absorption spectra of a 6624 h exposed sample: (a) surface; (b) inner region; (c) melt iPP.

than the inner material. During the ageing, band asymmetry and broadening decrease in the surface material, a phenomenon, which can be correlated to an enhanced degree of crystallinity near the surface. This conclusion can be better supported by comparison (Figure 13) among infrared spectra of: (13a) surface powder from a sample withdrawn after 6624 h; (13b) powders from the inner region of the same sample; (13c) melted unexposed iPP sample (at 190°C in a KBr pellet). Spectrum 13c is reported as a reference for a disordered phase, whose IR spectrum is expected to look very similar to that of amorphous iPP.

Several broad bands of the amorphous materials can be seen in semi-crystalline iPP under the sharp peaks characteristic of the crystalline phase (15–17). This is clearly shown in Figure 13, where the large bands of the melted iPP at 1380 cm^{-1} can be seen in semi-crystalline iPP as a broad component under the line of the crystalline phase. Components from an amorphous phase strongly decrease in the degraded materials giving rise to more sharp and symmetric bands.

Thermal Analysis

In this section the results of a series of thermal analysis (DSC thermograms and thermogravimetric measurements) carried out on iPP samples withdrawn after different times are presented. DSC experiments regarding:

i. The study of the *melting process* of different samples, followed by DSC experiments at a heating velocity of 20 deg min^{-1}. These experiments allow us to obtain trends of values of the melting enthalpy ΔH^{melt} with increasing the exposure time of the sample. These changes can be correlated to changes in the degree of polymer crystallinity. The same DSC curves show changes in shape and position of the maximum (T_{max}) of the melting peak. These characteristics can be correlated to the occurrence of crystallites of different stability, i.e., can reveal modification of the molecular weight distribution and of the amount of defective chains (19–22).

ii. The study of the *crystallization process* for samples exposed for different times. This study has been performed by cooling the previously melted samples at a velocity of 5 deg min^{-1}. According to these experiments, the enthalpy of crystallization can be measured. These data are complementary to the data of experiments i. They give information on the thermal behavior of the degraded samples when the memory of the morphology changes induced by the weathering is lost (by melting). These experiments are then related to the chemical modifications occurring in the samples during the outdoor exposure.

iii. The study of the *melting process* of the samples after recrystallization. The samples analyzed have been obtained by the following treatment: iPP plates at a different time of exposure have been melt and than recrystallized at a high cooling rate. As in the case of ii) also for these samples, the memory of the structural rearrangement during the exposure is lost and we can follow the only effect of chemical modifications.

Thermo-gravimetric analysis finally has been performed for samples withdrawn at different times.

Let us comment on the experiments from i) to iii) in detail:

i. Figure 14 shows the trend of ΔH^{melt}, while increasing the time of weathering of the sample. By interpolation of the experimental points, we find a "global" increase of ΔH^{melt}, which changes from about 85 Jg^{-1} to about 115 Jg^{-1} at 11640 h, thus exceeding the initial value of about the 40%. This increase can be correlated to an enhancement of the percentage of the crystallinity, which can be ascribed to several

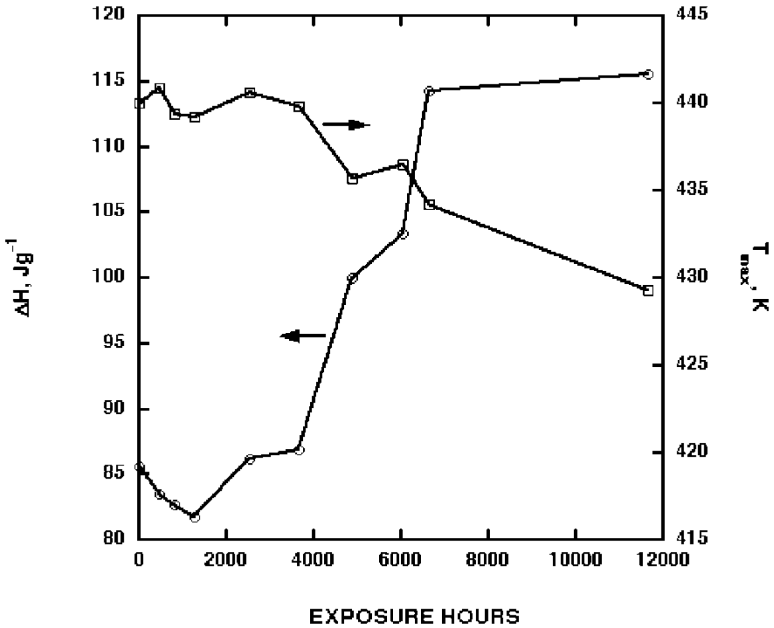

Figure 14. Melting enthalpy and T_{max} of iPP samples obtained by DSC curves (20 deg min^{-1}) vs. exposure time.

different processes, namely: a) degradation and "removal" of the amorphous phase, preferentially attacked by the oxygen; b) formation of new, low molecular weight species, which are able to form new crystalline domains; c) rearrangement of the starting morphology (characteristic of unexposed samples) by lamellae thickening, as an effect of the annealing due to the heating and cooling associated to the natural thermal excursions; d) thermally activated crystallization of defective chains (19–22). Process b) and d) can be correlated to the observed behavior of T_{max}, which shows a decreasing trend (a shift of about 10 degrees is observed from the pristine sample to the more exposed one), probably associated to the presence of less stable and chemically modified crystalline domains in the weathered samples. In a recent work (8), the enhancement ΔH^{melt} observed for iPP samples naturally weathered has been directly correlated to the increase of the crystallinity percentage by density measurements based on positronium spectroscopy. Notice, moreover, that the data reported in Figure 14 describes an irregular trend both in for ΔH^{melt} and T_{max}. Similar irregular trends have also been observed in Reference 7. In particular, it can be noticed that at the very beginning of the exposure (in a range of exposure times for which no oxidation phenomena can be detected, e.g. by infrared analysis) ΔH^{melt} shows a small but systematic decrease. This behavior, which cannot be ascribed to chemical modifications, has to be related to some morphology changes occurring in the first stage of the weathering. In order to better follow the evolution of the shape of the melting peak, we have performed some DSC experiments at the very low heating velocity of 2.5 deg min^{-1} (Figure 15). If we look to the curve obtained for a sample withdrawn after 816 h, we can observe a clear shoulder in the low temperature side of the peak. These features look like those previously observed in the case of a thin film of iPP, exposed in the same place (7). The

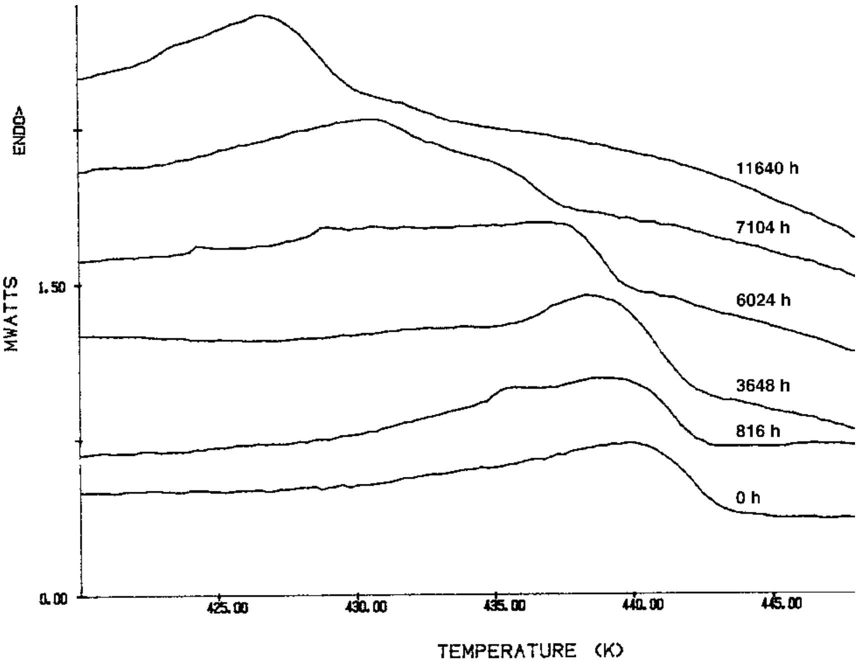

Figure 15. DSC curves of iPP samples (2.5 deg min^{-1}) withdrawn after different exposure times.

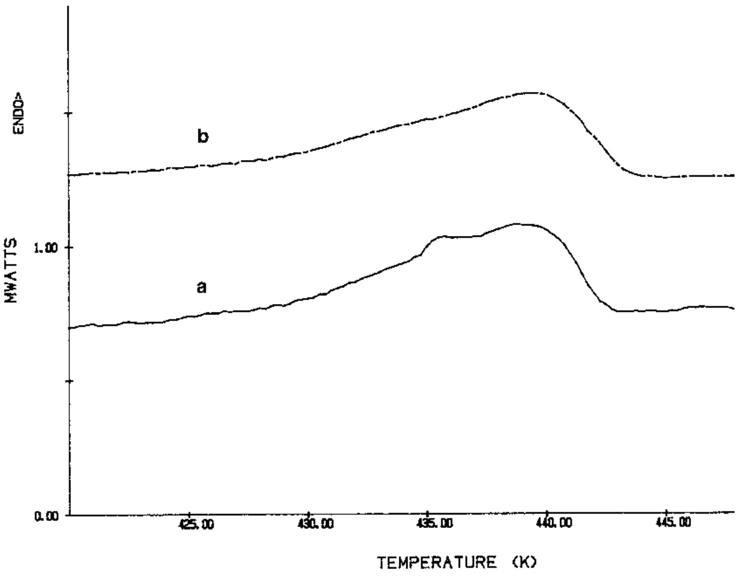

Figure 16. DSC curves of 816 h exposed iPP sample (2.5 deg min^{-1}): (a) before and (b) after annealing (1 h at 353 K), see text.

irregular shape of the melting peak become more and more pronounced as the time of exposure increases; after 6000 h, it shows "structures" also on the high temperature side. The irregular shape shown by DSC melting peaks can be ascribed to the formation (due to weathering) of different crystalline phases, characterized by different stabilities (20, 22). This conclusion can be supported by the experiment illustrated in Figure 16 where the DSC plot obtained for the sample withdrawn after 816 h is compared with that recorded for the same sample after a preliminary thermal treatment during which it has been heated (for 1 h) at 353 K. This pre-treated sample shows a much more regular shape of the melting peak. A similar result has been obtained with a sample exposed for 3648 h. These findings indicate that the "irregularities" shown in DSC plots of the weathered samples are due to the formation of new (heterogeneous) crystalline domains whose structures can reorganize under a moderate heat supply. On the other hand this consideration suggests that the meta-stable morphology of the exposed iPP samples can undergo important (dynamic) modification during the whole exposure time due to the thermal excursions associated to the days and nights cycles and to the seasonal climatic changes. In this regard, Figure 17 shows the wide range of variation of the minimum (plot a) and maximum (plot b) temperatures recorded during the time of exposure, in Messina (12). Thermal excursions which reach 20°C are observed during the same month.

ii. In Table 2 data are reported relative to the enthalpy of crystallization ($\Delta H^{\mathrm{cryst}}$) and T_{min} from DSC experiment of dynamic cooling (5 deg min^{-1}) performed starting from melt samples. Samples characterized by increasing times of exposure show very small variation of T_{min}; the value of $\Delta H^{\mathrm{cryst}}$, after an initial raise, shows a decreasing trend with a maximum variation from the initial value (for the sample exposed for 11640 h) of about 10%. Notice that the changes of T_{min} and $\Delta H^{\mathrm{cryst}}$ are quite negligible with respect to the variation of T_{max} and ΔH^{melt} observed

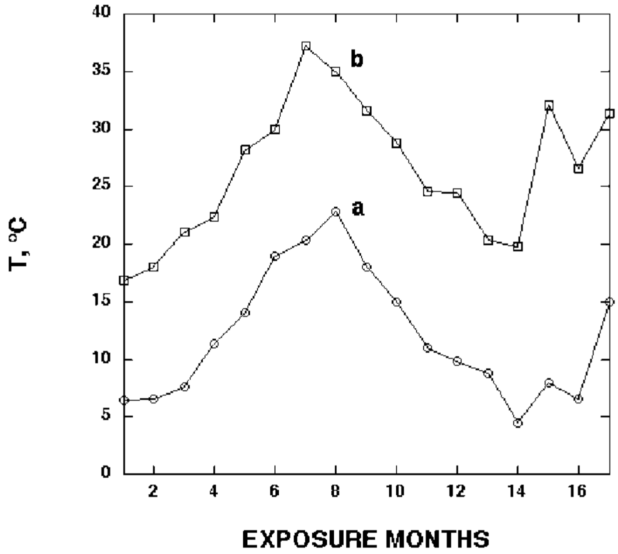

Figure 17. Monthly minimum and maximum temperature recorded in Messina during the exposure experiment.

(Figure 14) during the dynamical heating DSC experiments. Since, during the melting, the different samples have lost the memory of their morphology, these dynamic cooling experiments are, at least in principle, only sensitive to the different chemical composition of the sample (20). Accordingly, we can conclude that such a chemical modifications have a minor effect on the thermodynamic parameters (ΔH^{cryst}). On the other hand these data indicate that the large excursion in ΔH^{melt} observed by dynamical heating (see point i) is mainly due to relevant structural and morphological modifications induced during the outdoor ageing.

Table 2
Enthalpy of crystallization and peak temperature from DSC curves (cooling experiments) of exposed iPP samples

Exposure hours	ΔH ($-Jg^{-1}$)	T_{min} (K)
0	97.7	384.0
456	99.9	383.6
816	101.1	383.6
1272	97.9	383.0
2520	97.5	383.3
3648	96.8	383.7
4896	94.9	383.6
6024	91.3	383.3
6624	92.6	383.1
7104	89.9	382.9
11640	89.2	382.7

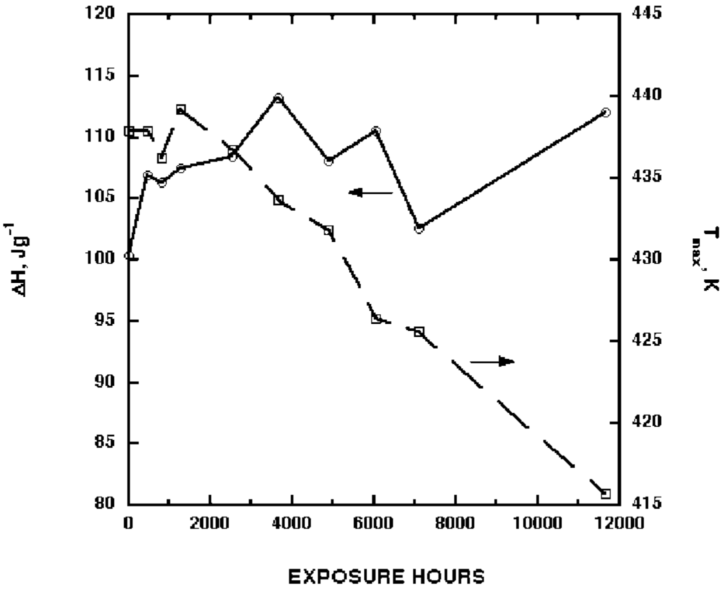

Figure 18. Melting enthalpy and T_{max} of iPP samples obtained by DSC dynamic curves (20 deg min^{-1}) after recrystallization (-320 deg min^{-1}) from the melt, vs. exposure time.

iii. Another set of experiments, which gives further support to the conclusions reached in ii, is illustrated in Figure 18. It shows the values of T_{max} and ΔH^{melt} obtained by DSC experiments on recrystallized samples. These samples are obtained from plates exposed for different times subjected to melting followed by rapid cooling (320 deg min^{-1}) (22). As expected, on the basis of the experiments described at point ii) one realizes that the ΔH^{melt} of the recrystallized samples oscillates in a narrow range (100–112 Jg^{-1}), while T_{max} shows a decreasing trend while increasing the weathering time, probably correlated to a reduction of the average molecular weight of the polymer.

During the natural ageing changes of the chemical nature of iPP are expected to take place, with formation of oxidation products (proven by infrared experiments) and degradation of the polymer. Figure 19 shows temperatures relative to the loss of 1% weight and 98% weight as obtained by TGA carried out on samples at different exposure times. In the 2500–7000 h range, the temperature required for reaching the 98% weight loss increases appreciably with the time of exposure of the sample. The results from TGA indicate that important modifications at the level of the chemical structure occurred at such a time of exposure, which must involve the whole bulk of the sample. The decrease of the temperature required for a 1% weight loss at high times of exposure (after 7000 h) suggests that a drastic reduction of the molecular weight (probably involving the chains near to the surface) takes place at these ageing times.

Chemical Degradation Mechanisms

The results obtained by the combined use of different techniques suggest that in the case of iPP, the chemical degradation proceeds with the oxidation of the first superficial layer of the plate where hydroperoxides are formed which easily give rise to alcoxy radicals (6).

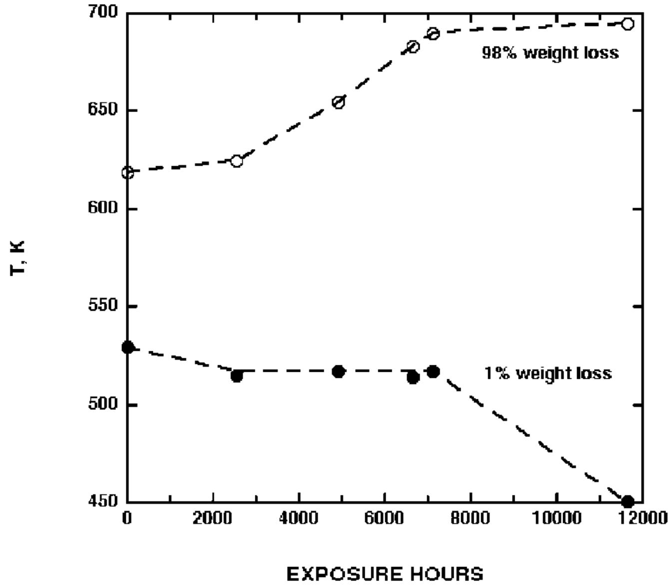

Figure 19. Temperature relative to the 1% and 98% weight loss of iPP samples obtained by dynamic thermogravimetric curves in air (20 deg min^{-1}) vs. exposure time.

These products can undergo decomposition with a β-scission reaction and a consequent decrease of the molecular weight of the macromolecules involved:

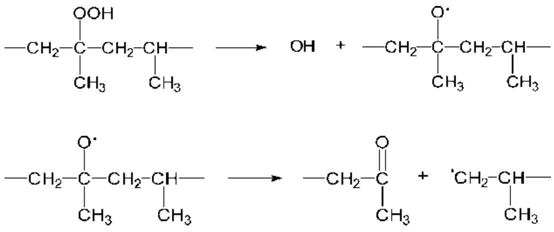

The macro-radicals originating from these reactions have low mobility in the solid iPP, but can transfer their radical activity to macromolecules in their neighbors. These macromolecules, in turn undergo decomposition (by a β-scission reaction) according to the following scheme:

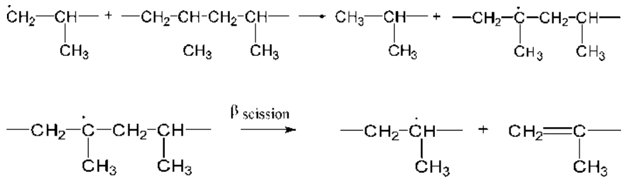

The formation of macro-radicals in the solid state and their successive decomposition (23, 24) can explain the fact that iPP degradation does not proceeds in a parallel way with the content of oxygen. Indeed, a mechanism which involves the formation of non oxygenated macro-radicals allows us to rationalize the fact that at high exposure times, the degradation process involves all the bulk material despite the fact that a modest content in oxygen is found in the inner region of the plates. This interpretation is in good agreement with the observations reported by Bedia et al. (2), which found a marked decrease in the polymer viscosity in correspondence with a relatively low carbonyl content.

Conclusions

Thick iPP plates, at different weathering stages, have been investigated with complementary techniques. A collection of many experimental findings bring us to the following conclusions.

From *ATR study of the surfaces* of the plates:

The oxidation processes on the surfaces start after a first induction time (at about 800 h of exposure no signals ascribed to oxygenated species can be detected) and increase until about 4000 h, after which a plateau is observed.

The iPP crystallinity percentage increases during the exposure and reaches a plateau after 6000 h;

These processes are more pronounced on the directly exposed surface.

From *infrared absorption* experiment:

Inside the plates, the oxidation processes start after 4800 h, and are less effective (lower intensity of C=O bands) with respect to what happens on the surfaces;

The crystallinity inside the plate continuously increases with the time of exposure;

Oxidation products and crystallinity percentage inside the plates are lower with respect to what was observed on the surfaces.

From *thermal analysis* we can conclude that the percentage of crystallinity shows a "global" increase according to ΔH^{melt} data from DSC analysis; however, some irregularities are found in the trend. The global increase is indeed supported by infrared data. Despite the fact that at 4000 h of ageing the degradation seems to be confined to the regions closer to the surfaces (as indicated by SEM analysis) the mechanical performances are drastically reduced at this time, with a change of the elongation at breaking from 528% (pristine un-aged sample) to 17%. It is important to notice that the degradation of the mechanical properties is observed at times of exposure when the content of oxygenated species is negligible especially in the inner region of the plates. This fact suggests that chemical reactions different from oxidation are responsible for chain degradation in the bulk of the material.

The behavior of the thick iPP plates observed in this work is different from what is found in the case of thinner films, whose natural weathering was studied with similar experiments, carried out in the same place (7). Indeed, in the case of iPP films, the crystallinity percentage, as deduced from DSC data showed a global decrease with the exposure time, while in the present work it shows an increasing trend.

In the case of thick samples, the existence of strong modifications at the level of morphology and crystal structure have been demonstrated both by infrared and DSC experiments. This structural rearrangement, which is not expected to have a simple and direct relationship with the formation of oxygenated species (mainly confined in a region near to the surface) largely dominates the thermal behavior of aged thick samples. On the opposite end, the behavior observed for the iPP films (7) can be mainly related to the chemical modifications (presence of oxygenated species and drastic reduction of the molecular weight) which, in a short time, would affect all the material, due to the low thickness of the samples.

References

1. Billingam, N.C. (2000) Degradation and stabilization of polymers. In *Material Science and Technology*; Cahn, R.W., Haasen, P. and Kramer, E.J. Eds., Wiley-VCH: New York; Vol. 19(II), 469–507.
2. Bedia, E.L., Paglicawan, M.A., Bernas, C.V., Berardo, S.T., Tosaka, M., and Kohjiya, S. (2003) *J. Appl. Polym. Sci.*, 87: 931–938.
3. Tidjani, A. (1997) *J. Appl. Polym. Sci.*, 64: 2497–2503.
4. Castejón, M.L., Tiemblo, P., and Gómez-Elvira, J.M. (2000) *Polym. Degrad. Stab.*, 70: 357–364.
5. Castejón, M.L., Tiemblo, P., and Gómez-Elvira, J.M. (2001) *Polym. Degrad. Stab.*, 71: 99–111.
6. Severini, F., Gallo, R., and Ipsale, S. (1988) *Polym. Degrad. Stab.*, 22: 185–194.
7. Gallo, R., Severini, F., Ipsale, S., and Del Fanti, N. (1997) *Polym. Degrad. Stab.*, 55: 199–207.
8. Brambilla, L., Consolati, G., Gallo, R., Quasso, F., and Severini, F. (2003) *Polymer*, 44: 1041–1044.
9. Girois, S., Delprat, P., Audouin, L., and Verdu, J. (1997) *Polym. Degrad. Stab.*, 56: 169–177.
10. Gugumus, F. (1998) *Polym. Degrad. Stab.*, 62: 245–257.
11. Wunderlich, B. (1976) Crystal nucleation, growth, annealing. In *Macromolecular Physics*; Academic Press: New York; Vol. 2, 149.
12. www.politicheagricole.it/ucea/forniture/index3.htm (accessed June 2003).
13. Scoolemberg, G.E. and Vink, P. (1991) *Polymer*, 32 (3): 432–437.
14. Scoolemberg, G.E. and Vink, P. (1991) *Polymer*, 32 (3): 438–444.
15. Natta, G. and Corradini, P. (1960) *Nuovo Cimento,* Suppl., 15: 40–51.
16. Zerbi, G. and Piseri, L. (1968) *J. Chem. Phys.*, 49: 3840–3844.
17. (a) Peraldo, M. and Farina, M. *Chimica e Industria*, (1960) 42: 1349–1361; (b) Peraldo, M. (1959) *Gaz. Chimica Ital.*, 89: 798–808.
18. (a) Carlsson, D.J., and Wiles, D.M. *Macromolecules*, (1971) 4 (2): 174–179; (b) Carlsson, D.J. and Wiles, D.M. (1971) *Macromolecules*, 4 (2): 179–184.
19. Rabello, M.S., and White, J.R. (1997) *Polymer*, 38: 6379–6387.
20. Rabello, M.S., and White, J.R. (1997) *Polymer*, 38: 6389–6399.
21. Elvira, M., Tiemblo, P., and Gómez-Elvira, J.M. (2004) *Polym. Degrad. Stab.*, 83: 509–518.
22. Guisández, J., Tiemblo, P., and Gómez-Elvira, J.M. (2005) *Polym. Degrad. Stab.*, 87: 543–553.
23. Lazar, M., Hrckova, L., Borsing, E., Marcincin, N., Reichlet, N., and Ratzsch, R. (2000) *J. Appl. Polym. Sci.*, 78: 886–893.
24. Becker, R.F., Burton, L.P.J., and Amos, S.E. (1996) Additives in polypropylene. In *Polypropylene Handbook*; More, E.P., Jr. Ed., Hanser Publisher: Munich Chapt. 4 181.